Biogeochemistry (2012) 110:269–285
DOI 10.1007/s10533-011-9669-9

Evaluating DMS measurements and model results in the Northeast subarctic Pacific from 1996–2010

Nadja S. Steiner · Marie Robert · Michael Arychuk · Maurice L. Levasseur · Anissa Merzouk · M. Angelica Peña · Wendy A. Richardson · Philippe D. Tortell

Received: 7 March 2011 / Accepted: 11 October 2011 / Published online: 3 November 2011

Abstract About a decade of dimethylsulphide (DMS) measurements in the North East Pacific are summarized and compared to model simulations. Bottle samples at various depths have been taken three times per year along Line P from the British Columbia coast to Ocean Station Papa (145° W, 50° N). Despite the long timeseries, DMS measurements are still sparse and the data show large variabilities in concentrations both spatially and temporally. DMS concentrations in late summer have been consistently high, while spring measurements at the offshore stations suggest a downward trend over the past years. Low values in spring, however, have also been recorded in the late 1990s, which might hint to interannual variability in the onset of the spring bloom and/or plankton assemblage rather than to a response to recent climate change. Some of the variability, both short-term and interannual, can be caused by regional or local preconditioning of the physical environment. The model simulations provide examples where periods of low winds, shallow mixed layers and sometimes high irradiance follow a mixing event and cause DMS peaks on various time scales as well as consistently elevated DMS concentrations for longer timeperiods. The model in its current configuration, which has been calibrated with measurements in the late 1990s/early 2000s, is not able to capture the low values in winter and spring observed in recent years. We suggest that this is due to missing or misrepresented links in the biogeochemical parameterizations of the model, e.g., an incomplete representation of variations in the phytoplankton assemblage. Including a seasonally varying S:N ratio to account for the absence of dinoflagellates in winter and spring significantly improves the simulation. Variability in DMS concentrations can also be induced by natural iron fertilization, which the model reproduces when timing is specified. For example, the model can reproduce the effects of natural volcanic Fe fertilization on surface water plankton dynamics and mixed layer DMS accumulation. The model also shows that the amplitude of the short term variability (days) increases when DMSP producing phytoplankton are less iron limited.

Keywords DMS measurements · DMS modelling · Marine sulphur cycle · Ocean Station Papa (OSP)

N. S. Steiner (✉) · M. Robert · M. Arychuk · M. A. Peña · W. A. Richardson
Institute of Ocean Sciences, Fisheries and Oceans Canada, Sidney, BC, Canada
e-mail: nadja.steiner@dfo-mpo.gc.ca

M. L. Levasseur
Department of Biology (Quebec Ocean), University Laval, Quebec, QC, Canada

A. Merzouk · P. D. Tortell
University of British Columbia, Vancouver, BC, Canada

A. Merzouk
University Laval, Quebec, QC, Canada

Introduction

Many questions are still open in terms of understanding the processes leading to the production of the biogenic gas dimethylsulphide (DMS) in the ocean and the links between sea–air DMS fluxes, atmospheric processes and global climate feedbacks. Even though the spatial coverage of DMS measurements has significantly improved over the last two decades (e.g., Lana et al. 2011), in depth studies and long term data sets which are essential to address the above questions (e.g., Halloran et al. 2010) are still sparse.

DMS is ubiquitous in the world's oceans but also highly variable (e.g., Belviso et al. 2004). Highest concentrations occur in summer in the southern ocean close to the Antarctic coast and in very localized areas in the Northeast and Northwest Pacific and the northern North Atlantic (Lana et al. 2011). Two of these areas (the southern ocean and the North Pacific) are also characterized by high-nutrient-low-chlorophyll (HNLC) water masses, where iron has been shown to play a major role in controlling primary production and phytoplankton community structure (e.g., Martin et al. 1989; Boyd et al. 1998, 2004).

The North East Pacific is an area with exceptionally high DMS production (which Wong et al. (2005) suggest to be a characteristic of the subarctic HNLC region), as well as high spatial variability on scales down to about 10 km (Asher et al. 2011). The region is home of one of the oldest timeseries stations in the world ocean (Ocean Station Papa, OSP, located at 50° N, 145° W, since 1949) and also provides one of the longest DMS measurement data sets (since 1996). Publications presenting and discussing the DMS timeseries at OSP and along Line P (Fig. 1) are still very limited, although research has been intensified since the subarctic ecosystem response to iron enrichment study (SERIES) in 2002 included an intense DMS measurement component (Levasseur et al. 2006; Merzouk et al. 2006) and model development (Le Clainche et al. 2006; Steiner and Denman 2008).

Wong et al. (2005, 2006) have summarized the measurements from 1996–2001. They find mean surface DMS values of 2 nM in winter, 6 nM in spring and 10 nM in summer, and respective average mixed layer concentrations (DMS_{MLD}) of 2.4, 8 and 16 nM. High DMS_{MLD} concentrations at the open ocean stations in spring and summer 1996–1998 were correlated with low chl-a_{MLD}. At OSP, Wong et al. (2006) report observed DMS concentrations (integrated over the mixed layer) in spring (summer) to be about 60 (40)% higher during the El Niño period (1997–1998) compared to the La Niña period (1999–2001). The ENSO event was characterized by warmer, more stratified waters with shallower mixed layers and higher abundance of phytoplankton species such as coccolithophores that are rich in dimethylsulfoniopropionate (DMSP), suggesting an influence of climate fluctuations on physical and chemical properties affecting phytoplankton assemblages and DMS concentrations in the upper ocean.

DMS in surface waters is formed via a complex network of processes (e.g., Stefels et al. 2007). The dominant process is suggested to be the release of dissolved DMSP ($DMSP_d$) triggered by phytoplankton cell lysis or leakage and zooplankton grazing. The DMS precursor, DMSP, is produced within the cells of certain species of phytoplankton. $DMSP_d$ is either transformed into DMS via bacterial or algal lysis, taken up by bacteria, or is transformed into dimethyl

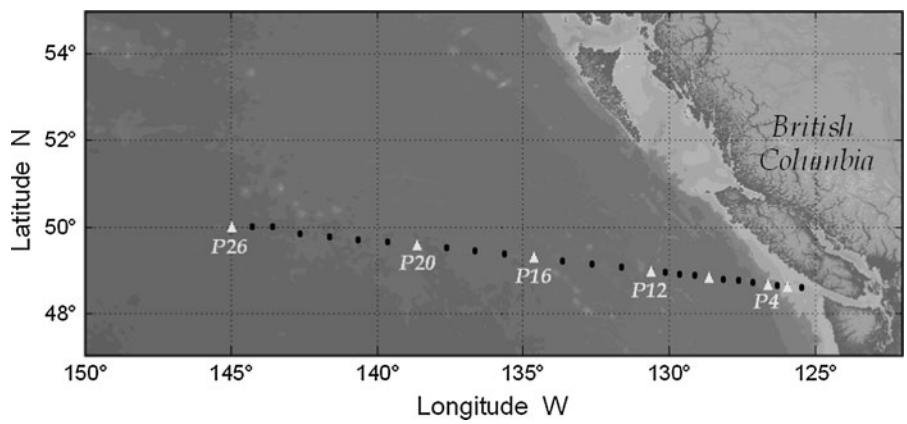

Fig. 1 Line P location in the Northeast Pacific from Vancouver Island to OSP (P26) located at 50° N, 145° W, showing the five main stations sampled along Line P

sulfoxide (DMSO) and other sulphur components (through demethylation and demethiolation pathways, e.g., see review in Schäfer et al. 2010). The DMS produced in the surface ocean is mostly consumed by bacteria or oxidized by sunlight (e.g., Schäfer et al. 2010) and some of it outgasses to the atmosphere.

Global modelling studies, mostly based on empirical parameterizations for DMS emissions, do not paint a clear picture in terms of DMS related feedbacks to climate change. Halloran et al. (2010) point out low skill levels for global models and advise caution in implementing DMS parameterizations into earth system models. Consequently, there remains a significant need for longer term data coverage and for the development of DMS parameterizations that realistically capture processes within the DMS cycle. Early results with a more sophisticated global DMS model (e.g., Six and Maier-Reimer 2006) hint to significant difficulties due to the complexities of the processes involved. A general issue is the high variability of turnover rates within the DMS cycle (e.g., Vézina 2004; Stefels et al. 2007), as well as the large spatial variability (e.g., Asher et al. 2011) which limits our understanding of processes as well as the development of parameterizations in DMS modelling efforts both on global and local scales (e.g., Campolongo and Gabric 1997; Cropp et al. 2004; Steiner and Denman 2008; Le Clainche et al. 2010).

The objectives of this paper are: (1) to summarize the last decade of DMS measurements in the vicinity of OSP and along Line P, (2) to compare more recent observations with those in the late 1990s and discuss both temporal and spatial changes in DMS concentration, (3) to test if the model which has been calibrated with the 1996–2001 data (Steiner and Denman 2008) can predict the more recent (2001–2010) observations and help understand the marine DMS system. We are aware that the data points are rather sparse, despite the length of the timeseries and that the results have a somewhat speculative character. However, we think it is important to make the data available for use and reference, to inspire discussion and thought processes, as well as to point out limitations of this kind of timeseries sampling.

In section "Background" we will outline physical and biological conditions of the study area and the measurement program along Line P and in section "Materials and methods" discuss the different measurements and methods as well as describe the model. Results will be presented in section "Results" followed by a summary (section "summary").

Background

Biology and physics of the study area

The usually iron-limited ecosystem at OSP shows chlorophyll values around 0.35–0.4 mg m^{-3} and small seasonal changes in phytoplankton biomass (e.g., Harrison et al. 1999; Boyd and Harrison 1999; Peña and Varela 2007). Algal biomass is dominated by small phytoplankton cells (<20 μm) mainly composed by prymnesiophytes, prasinophytes, cryptophytes, dinoflagellates and small pennate diatoms while most of the cells >20 μm are pennate and centric diatoms (Booth et al. 1993; Varela and Harrison 1999). Some of the common phytoplankton groups at OSP, such as dinoflagellates (e.g., *Ampidinium* spp., *Gymnodinium* spp. and *Prorocentrum minimum*) and prymnesiophytes (e.g., *Phaeocystis pouchetti* and *Emiliana huxleyi*) are recognized as significant producers of DMSP (Keller et al. 1989). Occasional iron input from varied natural sources can increase production significantly. Suggested sources for episodes of high production are dust inputs from Asia with a smaller contribution from Alaska (e.g., Boyd et al. 1998; Harrison et al. 1999; Moore et al. 2002) or volcanic eruptions (see section "Natural iron fertilization in September 2008" and Hamme et al. 2010). Additionally, nutrient-rich shelf waters can be transported to OSP via mesoscale eddies (e.g., Haida eddies forming off the Queen Charlotte Islands) or recirculating waters from the Alaskan Shelf (Whitney et al. 2005a, b; Johnson et al. 2005; Lam et al. 2006). Much of the water being carried into the open ocean lies below the euphotic zone resulting in iron enrichment in deeper layers ($\sim$1000 m) (Whitney et al. 2005b). With this mechanism of iron supply, the open ocean may become iron enriched for several years. Together with other nutrients, deep winter mixing can entrain iron into the surface mixed layer (Whitney et al. 2005b; Nishioka et al. 2001, 2003).

From a physical oceanography perspective, OSP, situated within the Alaska Gyre has been described as an ideal location for 1-D model studies: Horizontal advection is low (e.g., Denman and Miyake 1973) and a long timeseries of validation data is available. However variability in the Northeast Pacific is closely coupled

with events and conditions throughout the tropical and North Pacific Ocean, experiencing frequent El Niño and La Niña events particularly over the past decade (DFO 2009). Argo data from recent years illustrate processes that increase advection at OSP, e.g., shifts in the North Pacific Current (NPC) and the passage of eddies (Freeland and Cummins 2005; Jackson et al. 2006). The upper water column at OSP can be divided into two regimes with different mixing processes (e.g., Archer et al. 1993). The mixed layer immediately below the sea surface is maintained by wind generated turbulence. An annual cycle occurs due to the formation of a seasonal thermocline in summer, and at OSP wind stress curl causes a net upwelling of waters from below. Additionally, wind driven currents in the mixed layer may contribute fluxes of salt and nutrients. Below the depth of the winter mixed layer ($\approx$90 m), waters are stratified by a salinity density gradient (halocline).

The Line P program

Originally a weather station (since 1949), OSP became an oceanographic station in 1956. In 1959 12 stations were added along the line, and since 1981 27 stations (Fig. 1) are regularly sampled. Line P cruises are organized by the Department of Fisheries and Oceans (DFO) Canada three times per year, in winter (February), late spring (June), and mid/late summer (August). Before 1997, the spring cruise used to be in May and the late summer cruise used to be in September. The 2002 spring cruise was in July rather than June. The late summer cruise usually falls into late August or early September, depending on available ship time. Here the exception is in 2006 when the cruise had to be shifted to late September because of a ship refit. The regular June cruise in 2006 had to be cancelled due to delays in the ship yard, hence there is no DMS data for spring 2006. A summary of the collection frequency is shown in Fig. 2.

During a regular program, sampling at the five major stations (Fig. 1) includes DMS at 0, 5, 10, 15, 20, 25, 30, 40, 50, 75, 100, 175, 200 dbar. Sampled with the DMS are nutrients, chlorophyll (to 100 m), DMSP-t and DMSP-d (5, 10, 20, 100, 175, 200 dbar). Since 2006, high performance liquid chromatography (HPLC) samples have been regularly collected at 5, 10, 25 dbar for the measurement of phytoplankton pigments, which are used to estimate the contribution of each phytoplankton

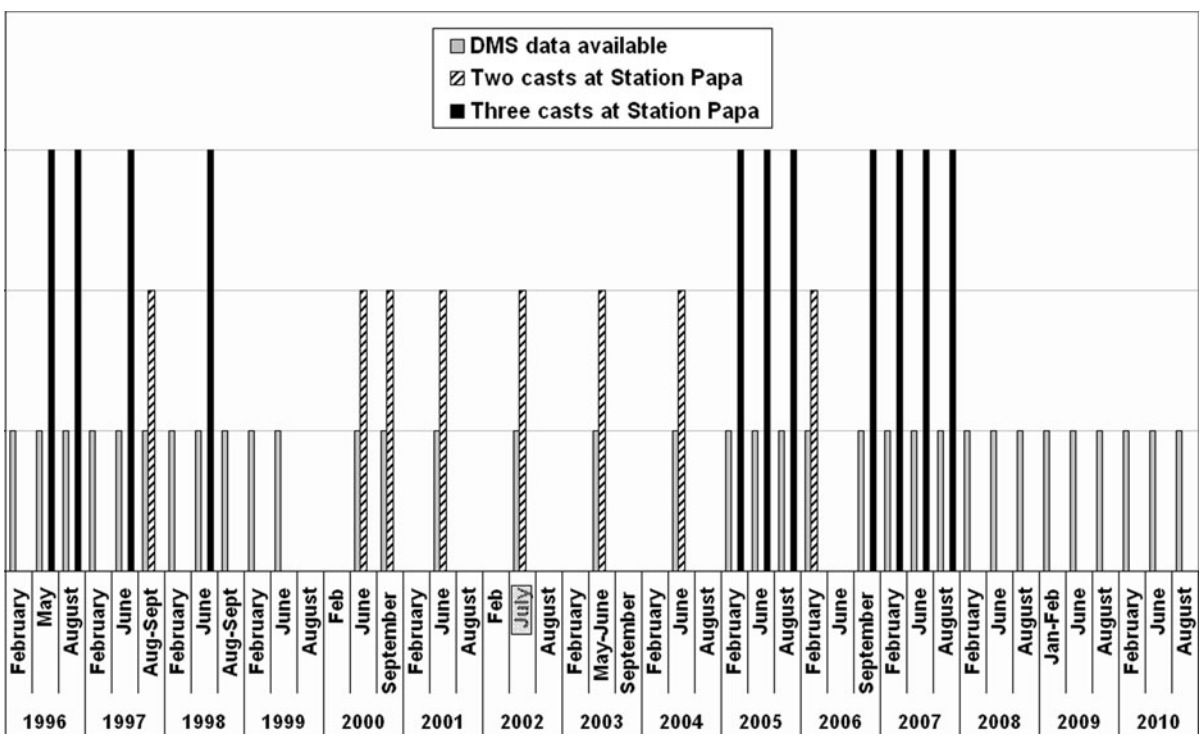

Fig. 2 DMS data availability at OSP from 1996 to 2010

group to chl-*a* biomass as described in Royer et al. (2010). Additionally, the CTD provides temperature, salinity, transmissivity, fluorescence, dissolved oxygen and photosynthetically active radiation (PAR).

Materials and methods

DMS measurements

DMS bottle casts have been regularly performed once per day, but occasionally samples have been collected more frequently to examine diurnal variability. (e.g., three casts per day in the upper ocean, if possible at local sunrise, noon and sunset, Fig. 2). Subsurface sea water samples were drawn from the Niskin samplers directly into 250 mL glass bottles which were then stored in the dark until analyzed. Analysis via a purge and trap system in the ship's laboratory began immediately after sampling. The method described in Wong et al. (2005) has been slightly updated. For the purge and trap system a 20 ml water sample is loaded into a stripping vessel and purged with UHP nitrogen for 10 min at 100 ml min^{-1}. The purge flow goes through a 4°C condenser that effectively removes all moisture from the sample stream. The DMS is extracted and absorbed onto a Tenax TA trap kept at −80°C. The trap is subsequently desorbed at 100°C onto a chromasorb 330 column, located in a gas chromatograph held at 40°C, and then eluted into a flame photometric detector (FPD). The primary standard was prepared once a week from a stock solution of DMS (Aldrich 471577) in isopropanol. The intermediate and working standards were made up fresh daily in double Milli-Q water and run immediately before analyzing each station profile. The system has been running since the late 1990s. In 2002 and 2003 the system was rebuilt and underwent a mid-life refit in June 2006.

Since 2007 additional measurements of surface water DMS concentrations have been made using membrane inlet mass spectrometry (MIMS) for high spatial resolution. The method has been developed at the University of British Columbia and is described in detail in Tortell (2005) and Asher et al. (2011).

Model description

The 1-D coupled model consists of atmospheric (ASCM) and oceanic (OSCM) single column models, where the latter includes a seven-component marine ecosystem model (Denman et al. 2006), with inorganic carbon, nitrogen, oxygen, and silica sub-models as described in Steiner et al. (2006, 2007). More recently sulphur cycling has been added (Steiner and Denman 2008, denoted as SD08 in the following). The ASCM is a single column model based on the atmospheric general circulation model referred to as AGCM4 (von Salzen et al. 2005). Temperature and humidity are nudged to National Center of Environmental Prediction (NCEP) reanalysis data (Kalnay et al. 1996) with a 3-day restoring time scale. Vector winds at all levels are specified from the same data set. The ocean component is the 1-D marine boundary layer model GOTM 3.0, (Burchard et al. 1999, see http://www.gotm.net) with configurations and modifications as described in Steiner et al. (2006, 2007). The vertical domain is 120 m with 1 m resolution. Temperatures and salinities over the whole domain are restored to observations from nearby Argo floats with a 30 day restoring time scale. For the bottom 10 m, the restoring time scale is set to 1 day.

The ecosystem model includes small (<20 μm, P_1) and large (>20 μm, P_2) size classes of phytoplankton, microzooplankton (Z_1), detritus (D), nitrate (N_i) and ammonium (N_a). Mesozooplankton (Z_2) are preset to an annually repeating daily climatology based on long term observations at OSP. Ecosystem variables are expressed in terms of the equivalent concentration of nitrogen with fixed ratios connecting the carbon and oxygen modules. The specific growth rate of phytoplankton is limited by light, nitrogen, iron, and for P_2 silicate. Iron limitation is represented by a constant parameter except for fertilization simulations (Steiner et al. 2006, SD08). This parameter represents the maximum growth rate under iron limitation as a fraction of the maximum specific growth rate ($L_{Fe_1} = 0.4$ for P_1 and $L_{Fe_2} = 0.2$ for P_2). In Monahan and Denman (2004) growth rates for small and large phytoplankton are the same with $L_{Fe} = 0.26$. In Denman et al. (2006) $L_{Fe_1} = 0.6$ and $L_{Fe_1} = 0.2$. We will be testing the sensitivity to the iron limitation in this study. All growth, grazing and lysis rates are temperature-dependent. Nitrate and silicate are relaxed to a constant profile in the bottom 30 m on a daily time scale. Attenuation of incoming solar radiation depends on the concentration of phytoplankton ($P_1 + P_2$), detritus (D) and a 40% contribution of

microzooplankton (Z_1) as described in SD08. Ecosystem parameter values are listed in Steiner et al. (2006) (their Table 3) with phytoplankton lysis rate as in SD08. Following observations at OSP, we can make the simplifying assumption that $DMSP_p$ is only produced by small phytoplankton P_1. The processes represented in the sulphur model are: the release of $DMSP_d$ via algal lysis, leakage and microzooplankton grazing as well as direct release of DMS during these processes (during grazing some DMSP*p* is allowed to be lost, forming DMSO and other sulphur components (S_p) which are not represented explicitly); bacterial consumption of $DMSP_d$; bacterial and enzymatic cleavage to DMS; air–sea exchange; photolysis and bacterial consumption of DMS. The model parameters which represent individual conversion and turnover rates in the marine sulphur system are usually determined via measurements. Unfortunately, measured turnover rates vary significantly (see section "Introduction"). While the chosen model parameters lay within the observed range a reasonable value within this range needs to be chosen. This is usually done by slightly adjusting the parameters to match the model variables with an available measurement data set (model tuning). In this case the observations described in Wong et al. 2005 have been used to tune the model parameters. (See SD08 for a more detailed description, model equations and parameter values). SD08 show in their sensitivity study that DMS production is most sensitive to variations of the intracellular S($DMSP_p$):N ratio (in mg-S per mg-N) within phytoplankton ($q = 0.45$) and the bacterial consumption rate of DMS, which will be discussed further in section "Simulated annual cycle at OSP". The model also uses the variable DMS yield (ratio of bacterial DMS production to bacterial uptake of DMSPd) introduced in SD08.

The model has been integrated from March 2002 to September 2010 where acceptable coverage of Argo data in the vicinity of OSP allows restoring to realistic values.

Results

Spatial and temporal variability along Line P

Figure 3 shows the DMS concentration at the surface along Line P for spring and summer as obtained via bottle measurements from 1996 to 2010. These measurements show high temporal and spatial variability. Averages presented in Wong et al. (2005) are likely influenced by high values during the strong El Niño in 1997–1998 (Wong et al. 2006). Subsequently, a link to the El Niño Southern Oscillation (ENSO) or Pacific decadal oscillation (PDO) is much less obvious. In spring a general decrease in concentrations can be seen since 1997/1998 with more recent data showing low values similar to what has been measured in 1996 before the El Niño. In summer the picture looks somewhat different. While the concentrations after the 1997/98 El Niño (in 2000, 2005 and 2006) were exceptionally low, they have returned to much higher values in recent years, again more consistent with the 1996 measurements. The exceptionally high values at some stations in 2008 are likely caused by an anomalous plankton bloom fuelled by volcanic ash (Hamme et al. 2010) (see section "Natural iron fertilization in September 2008").

Spatial variability along Line P can partially be attributed to the presence of two distinct and contrasting environments (Royer et al. 2010; Asher et al. 2011): The nutrient-rich diatom dominated inshore waters and the Fe-poor prymnesiophyte-dominated offshore waters. Royer et al. (2010) find that the offshore HNLC stations were characterized by higher DMSPp:chl-*a* ratios as well as higher DMS yields and lower DMSP-S assimilation efficiencies. This suggests that bacteria have a greater proportional use of DMSP as carbon source rather than a sulphur source under HNLC conditions, which has also been found during the SERIES experiment (Merzouk et al. 2006).

The data indicate that regional spatial variability at the surface (1–13 nM in June and 1–17 nM (Bottle) and 1–69 nM (MIMS) in August 2008) along Line P can exceed interannual variability, obscuring long-term trends. In 2007 and 2008 the open ocean surface DMS concentrations remained low in June, whereas high DMS fronts could be observed in August. While Wong et al. (2005) find an increase in DMS concentrations from coastal stations to the open ocean regime, June measurements by Royer et al. (2010) show lower values at the offshore stations and Asher et al. (2011) find that the longitudinal concentration gradient reverses seasonally, with highest values accumulating in offshore waters during summer. Data plotted in Fig. 3 confirm this reversal for most years both before and after 1997/1998. We suggest that the

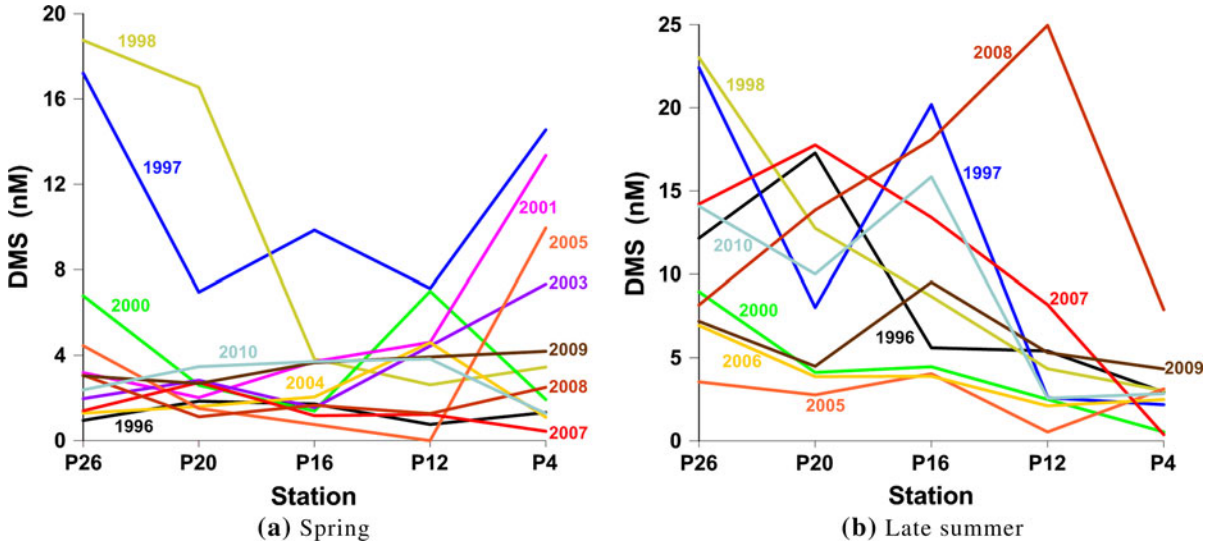

Fig. 3 Spatial and temporal variability of observed surface DMS (nM) along Line P in: **a** spring (May/June), and **b** late summer (August/September). Line P cruises are three times per year, in winter (February), spring, and late summer. Before 1997, the spring cruise used to be in May and the summer cruise in September. The spring cruise is now in June (July for 2002), and the late summer cruise usually falls into late August or early September, depending on available ship time (An exception is 2006 when the cruise had to be shifted to late September)

increase from coastal to offshore stations is generally a trademark of the summer condition and occurs in spring only under a strong El Niño influence.

Variability at OSP

Observed interannual variability at OSP in spring and summer can be seen in the variety of vertical profiles from 1996 to 2010 (Fig. 4). Generally, elevated DMS concentrations are limited to the euphotic zone, where phytoplankton produce the precursor DMSP and most of the DMS production and degradation takes place. Concentrations significantly decrease below 40–50 m and reach values close to the detection limit below 70 m. One characteristic of DMS profiles during periods of high production is the subsurface maximum, located between $\sim$15 and 40 m depth.

Figure 4a shows measurements in spring (May/June) at OSP. While exceptionally high DMS concentrations have been measured during the El Niño years 1997 and 1998 (15–25 nM in the top 10 m), the somewhat higher concentrations ($\sim$4–8 nM) observed in 2000, 2002 and 2005 seem rather an exception (note that 2002 measurements are from the July 2002 cruise before the SERIES experiment commenced). The low concentrations (<4 nM) seen in the last 4 years are consistent with measurements in 1996, 1999, 2001, 2003 and 2004 and possibly more representative for spring conditions. In summer (Fig. 4b), we generally observe the highest DMS concentrations. 1997 and 1998 are still the highest, however the difference in concentrations with other years is much less pronounced than in spring. With some consistency the highest values in summer occur in the same years as the low values in spring, e.g., 1996, 2007, 2009 and 2010, which likely indicates a late bloom of DMSP producing phytoplankton species. Unfortunately there are no summer profiles for 1999, 2001, 2003 and 2004. 2008 values are comparatively low. However in view of the volcano triggered anomalous plankton bloom initiated just a week before the ship measurements (see section "Natural iron fertilization in September 2008") the small phytoplankton bloom has likely been triggered earlier and more intensely, causing high zooplankton grazing. While zooplankton grazing causes release of DMSPd it eventually leads to the crash of the bloom leading to a reduction in the DMS production. These characteristics have been modelled and observed for the SERIES experiment as a response to iron enrichment (Levasseur et al. 2006, SD08). The lowest summer concentrations have been measured in 2005 and 2006. 2005 is in fact a year where higher values in spring have been encountered. The latter can likely be related to increased stratification and shallow

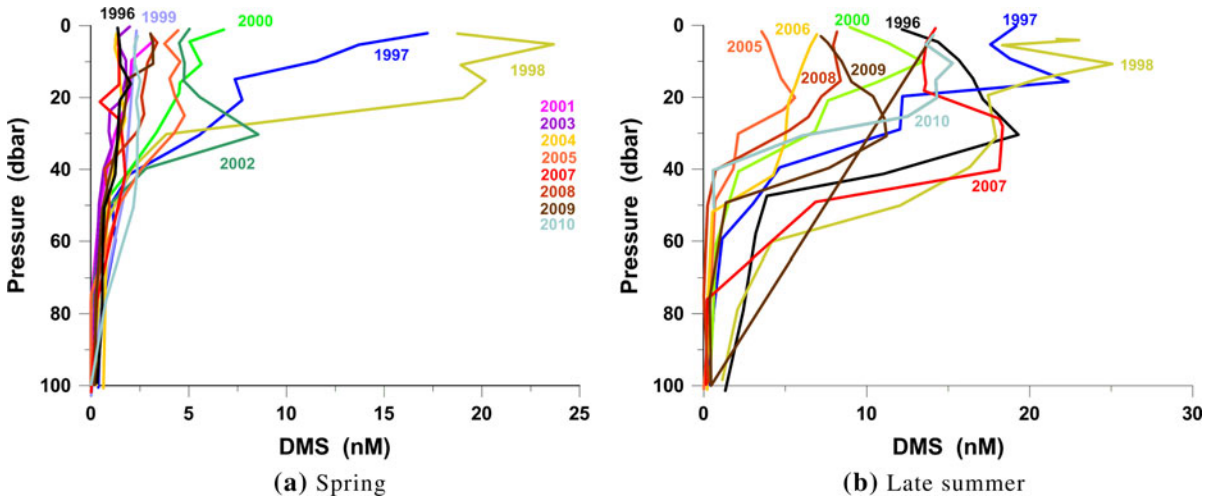

Fig. 4 Vertical profiles of DMS (nM) at OSP from 1996 to 2010 in: **a** spring (May/June), and **b** late summer (August/September). Cruise timing as in Fig. 3

mixed layers linked to a particularly high PDO signal that year (see model discussion, section "Simulated annual cycle at OSP"). No measurements are available for spring 2006, but the summer cruise was in late September that year and is not representative for summer conditions. The year 2000 shows neither very low values in spring nor very high values in summer.

Asher et al. (2011) found significant correlations of surface DMS concentrations with some variables (calcite, chl-*a*/MLD ratios and irradiance), but they were unable to produce a single consistent empirical relationship predicting surface DMS. In the current data set, we could not find any significant relationships to variables such as temperature, salinity, oxygen or nutrients other than the obvious depth related trends. (Links to wind speed, irradiance and MLD are discussed in section "Simulated annual cycle at OSP"). Connections to phytoplankton assemblages can be studied using HPLC measurements of pigment analysis of marine phytoplankton which are now available for some of the recent years. Figure 5 shows the contribution of main phytoplankton groups to chl-*a* biomass as estimated from the concentration of biomarker pigments from June 2006 onward. Relative contributions of diatoms, prasinophytes, cryptophytes and high DMSP producing prymnesiophytes and dinoflagellates are shown. It can be seen that in late summer, when high DMS production is frequently observed, prymnesiophytes and dinoflagellates are the dominant phytoplankton groups representing on average, 47 and 30% of the total chl-*a*, respectively. The relative contribution of diatoms is usually very low (<5%). An exception is 2008 where diatoms are present following natural iron input (see section "Natural iron fertilization in September 2008"). In winter, the contribution of other phytoplankton groups increases. Prymnesiophytes still dominate phytoplankton biomass, but dinoflagellates are notoriously less abundant. Hence, the ratio of DMSP producers to non-DMSP producers within the small phytoplankton group is higher in summer (DMS producers are about 90% of P_1) than in winter and spring (DMS producers are <50% of P_1). In general primary production is low in winter and DMS concentrations are close to zero. During the spring, the contribution of diatoms increases, becoming also dominant while other phytoplankton groups continue with relative contributions at winter levels; primary production increases and DMS production starts to pick up. An exception is 2008, where diatom contributions remain relatively low and prymnesiophytes significantly increase. However, dinoflagellate contributions remain insignificant and DMS concentrations are only slightly higher than in other years. In summary, it can be suggested that DMSP producing phytoplankton species are low in spring (May/June) and only bloom later in the year linked to highest DMS production rates in late August/early September. Later in September the DMS peak is either reduced to a subsurface signal or generally declined. In occasional years, possibly linked to PDO or ENSO, a phytoplankton bloom might be triggered earlier in the year causing increased DMS

concentrations already in spring. In those years DMS concentrations are lower in August, which is more characteristic for fall.

The results are still quite speculative. While a 10–15 year timeseries seems long, inconsistencies in cruise timing make it hard to track down interannual signals. Moreover, horizontal variability in surface DMS is quite large. Asher et al. (2011) calculate a length scale of less than 10 km for DMS variability, which suggests that extremely high values which are occasionally detected at OSP are spatially limited and might not necessary be captured in every year.

Simulated annual cycle at OSP

The simulated annual cycle of DMS from 2002 to 2010 is shown in Fig. 6a. Model parameters have been tuned to fit observations from 1996–2001, published in Wong et al. (2005) (see section "Model description"). For reference, monthly averaged observations by Wong et al. (2005) for the available months are plotted as triangles in years 2002 and 2003. The large error bars, specifically in summer, are indicative of a large variability which we also see in the newer data. The modelled annual cycle fits the 1996–2001 observations well (see also SD08). However, observations in recent years don't confirm the modelled annual cycle. Figure 6b shows the simulated mean (2002–2010) annual cycle (solid black line) with observations (symbols, see figure caption). Fig. 6c shows correlations between the simulated mean monthly DMS concentrations and the respective observations. Again, the averages presented by Wong et al. (2005) are reasonably close to the observations (triangles), as are the averaged MIMS data in August (diamonds). However, bottle measurements (asterisks: 1996–2001, crosses: 2002–2010) show large variabilities and significantly lower values in June, more obviously in recent years. The model data correlation is generally unsatisfactory. Winter (February) observations are significantly lower for recent years, which is not captured in the model. While the concentrations varied between 1 and 3 nM in the late 1990s and early 2000, they are close to the detection limit (below 1 nM) in recent years. No changes affecting the detection limit or which could otherwise explain these changes have been made to the instruments. Hence, the reason for these low numbers is still unclear and will need further investigation over the coming years.

Changes in the annual cycle and/or differences between model results and observations can be caused by: (1) Changes in the physical environment (forcing, see section "DMS response to physical forcing"); (2) Changes or misrepresentations in turnover rates (production, loss) within the marine sulphur cycle. (3) Changes or misrepresentations in the plankton community structure; both of the latter will be discussed in section "Model sensitivity studies".

DMS response to physical forcing

The model is restored to observations which represent interannual changes in physical variables (temperature, salinity, wind, humidity). Hence, significant changes in the physical environment will be represented in the model forcing and respective DMS responses should be seen in the model. However, monthly averaged model output (Fig. 6b) indicates

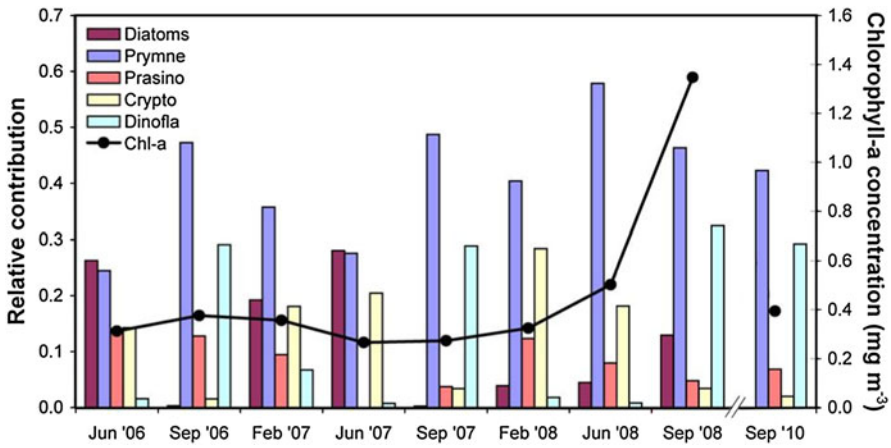

Fig. 5 Chlorophyll-*a* concentration (mg m^{-3}, *right axis*) and relative contributions of prymnesiophytes, dinoflagellates, prasinophytes, cryptophytes, and diatoms to total chl-*a* (*left axis*) at OSP from phytoplankton as determined from HPLC pigment analysis for several cruises from June 2006 to September 2010

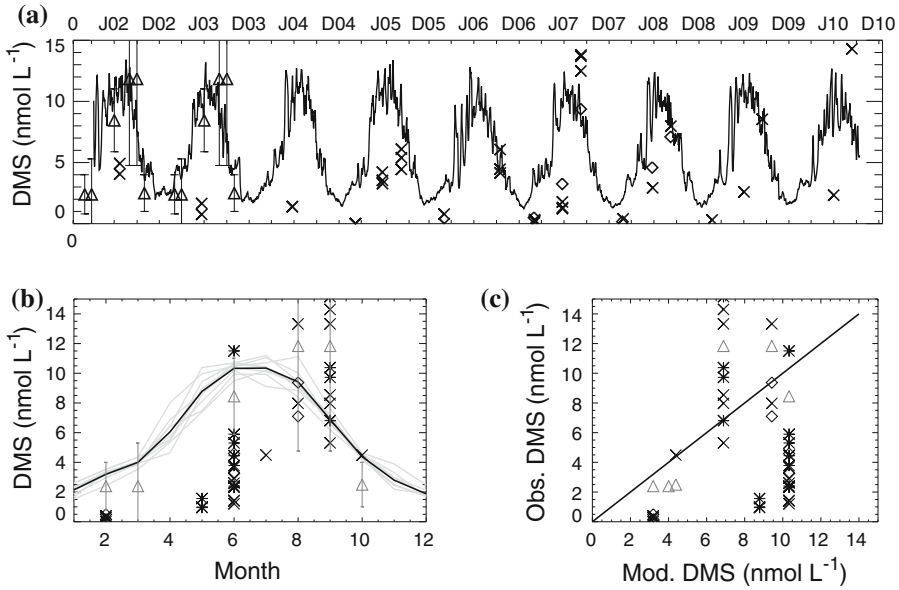

Fig. 6 **a** Simulated annual cycle of DMS (nmol l^{-1}—averaged over the top 20 m), from 2002 to 2010. Model parameters (SD08) have been calibrated based on observations published in Wong et al. (2005). Latter are plotted in years 2002 and 2003 (*triangles*) for comparison. Recent observations are overplotted at the appropriate time (*crosses* bottle casts, *diamonds* MIMS data averaged for the vicinity of OSP). **b** Simulated mean annual cycle of DMS (nmol l^{-1}—averaged over the top 20 m) for the years 2002–2010 (*solid black line*, *grey lines* show individual years). Observations are plotted as symbols in the month they have been measured (*diamonds* MIMS, *triangles* bottle casts 1996–2001, *crosses* bottle casts 2002–2010, *asterisks* averaged monthly values as provided by Wong et al. (2005)). **c** *Scatter plot* of modelled DMS versus observed DMS: each observed value is assigned to the simulated monthly mean value as shown in **a** (*black solid line*)

only very limited interannual variability in the DMS concentration (e.g., 2005, 2006, see below) and does not show a significant change in the annual pattern which could cause the observed decline in spring DMS concentrations. On shorter timescales, however, a link between the physical conditions (wind, temperature, stratification) and DMS response becomes apparent. Incoming shortwave radiation and wind speed as seen by the model and simulated mixed layer depth, (both as determined via a turbulent kinetic energy (tke)-criterion and a temperature criterion, see figure captions) are shown for 2005–2006 in Fig. 7c–e. For example in 2005, a combination of early high irradiances (highest in the 2002–2008 timeseries), low winds and shallow mixed layers leads to fairly continuous higher than usual DMS concentrations during May and June that year (Fig. 7b), which is also seen in the observations (see above). On the other hand, spring 2006 is characterized by a series of strong wind and deep mixing events. After each mixing event, a short episode of calm winds and shallow mixed layers leads up to a peak in DMS concentration (indicated by vertical lines in Fig. 7b–e).

A correlation with PDO and ENSO indices (not shown) relates high observed DMS concentrations in 1997/1998 to the strong El Niño signal in 1997/1998 and La Niña in 1999 as discussed in Wong et al. (2006). After that, observed DMS concentrations are lower and PDO/ENSO indices enter a negative phase. Short term increases in the decadal climate signals occur in winter 2002 and spring 2005. As discussed before, spring 2005 did in fact show stronger stratification and shallower mixed layers in spring, causing higher phytoplankton and DMS production. We conclude that DMS concentrations show a response to decadal climate signals like the PDO or ENSO only in years with exceptionally high indices, but a more general correlation cannot be found. In summary, the results suggest that the observed lower winter and spring values are not caused by changes in the physical forcing.

Model sensitivity studies

Rather than based on the physical forcing, the winter and spring overestimation in recent years might be of

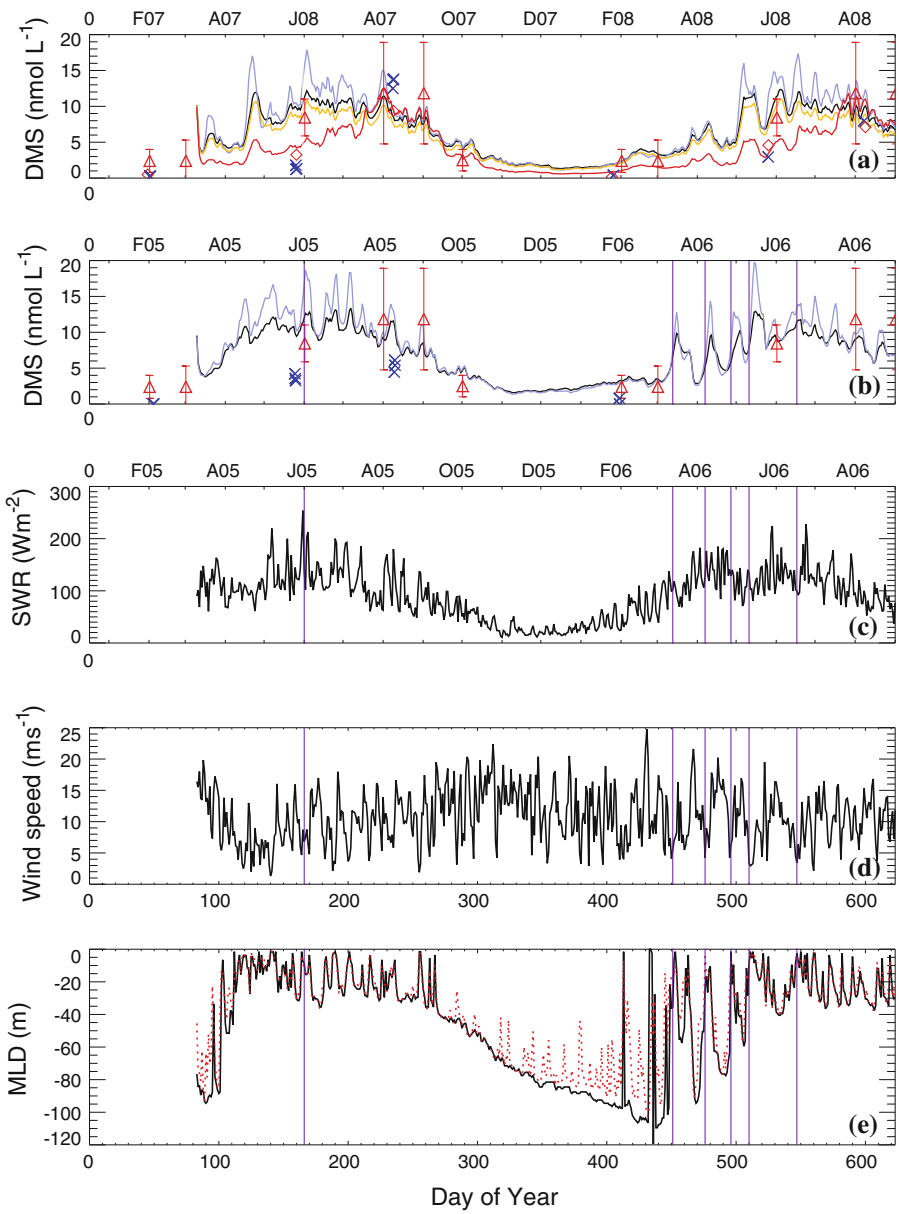

Fig. 7 **a** Simulated DMS (nmol l^{-1}—averaged over the top 20 m) from March 2007 to September 2008 for the standard run (*black line*, parameterization as in SD08 and for simulations with reduced iron limitation (*blue line*, $L_{Fe_1} = 0.6$ for P_1), with reduced S:N ratio (q = 0.4, *yellow line*), and with seasonally varying S:N ratio based on dinoflagellate abundance (q = 0.2–0.5, *red line*), see text. **b** *Black* and *blue line* as in **a** but for 2005–2006. Averages of earlier measurements by Wong et al. (2005) (*triangles*) and recent observations are overplotted at the appropriate time (*crosses* bottle casts, *diamonds* MIMS data averaged for the vicinity of OSP—2007/2008 only). Physical variables are presented for 2005–2006. **c** Shortwave radiation from NCEP reanalyses as seen by the model (W m^2), **d** simulated wind speed (m s^{-1}) and **e** simulated mixed layer depth using a temperature criterion ($T_{MLD} - T_{surf} > 0.1$°C, *solid line*) and a turbulent kinetic energy criterion (tke > $10^{-5}m^2\ s^{-2}$ *dotted line*). *Vertical lines* indicate the beginning of a peak in DMS concentration in correlation with low winds and shallow mixed layers (and high irradiance) following a recent mixing event (days 166, 451, 476, 496, 510 and 547)

biological nature. To further discuss possible inadequacies in the current model configuration, we performed several sensitivity studies. The yellow line in Fig. 7a indicates a run with reduced cellular S:N ratio for small phytoplankton ($q = 0.4$, see section "Model description"). While this leads to a reduction

of DMS concentration, more pronounced in spring and summer, it is not sufficient to explain the observed spring decline. A similar result is obtained when increasing the bacterial DMS consumption rates (not shown). Differences between the model and observations might also be caused by a misrepresentation or possibly shift in the phytoplankton assemblage. HPLC analyses show a lower ratio of DMSP producing to non-DMSP producing phytoplankton species within the small phytoplankton group in winter and spring compared to summer due to the absence of dinoflagellates. This suggests that the S:N ratio (q) within the modelled small phytoplankton group is not constant over the year. Based on the HPLC results (section "Variability at OSP") a test run has been performed where q has been set to a wintertime value of $q_w = 0.2$. In August and September, q is set to 2.5 q_w and in July and October q is set to 1.5 q_w as an intermediate value (red line in Fig. 7a).

The results clearly show a reduction in simulated winter and especially spring concentrations while summer values remain at former high values. Figure 8a, b show a revision of Fig. 6b, c, using the discussed model run with seasonally varying q. The simulated winter and spring values are significantly lower and the interannual variability of the summer maximum is slightly increased, leading to an improved model-data correlation. These results identify the lacking separation of prymnesiophytes and dinoflagellates in the model as a likely cause for the overestimation of simulated DMS concentrations in winter and spring.

The fixed large zooplankton representation in the model might be another issue. Observations show significant changes in copepod abundance with climatic shifts in the Northeast Pacific, with smaller copepods being more important in warmer years (especially 2005) and higher abundances of large copepods in cooler years (e.g., DFO 2009; Mackas et al. 2006). A simple test simulation with a shifted cycle in large zooplankton (not shown) confirms a response of the planktonic system and DMS production: With maximum zooplankton production later in the year, DMS production in spring is somewhat reduced and slightly higher in late summer. While the magnitude of the change is not sufficient to explain the difference between model and observations, changes in zooplankton assemblages might contribute to interannual variabilities, which are not represented in the model.

Blue lines in Fig. 7a and b show simulations with a weaker iron limitation (from $L_{Fe_1} = 0.4$ to $L_{Fe_1} = 0.6$). It can be seen that releasing the iron limitation leads to an increased amplitude of the DMS variability. The simulated DMS concentration becomes much spikier. The largest spikes occur during calm periods with shallow mixed layers and—often, but not always—increased shortwave radiation, following a mixing event. This is most prominent in spring, when waters are enriched in nutrients following deep winter mixing (e.g., beginning at day 166, 451, 476, 496, 510 and 547—vertical lines in Fig. 7). This combination of physical precursors can be very localized and short term and could explain some of the high temporal and spatial variability observed in the region. For example, Asher et al. (2011) show in their Fig. 10a, a pronounced DMS peak in correlation with low winds and increased shortwave radiation on a timescale of several hours.

At OSP, presumably winter mixing also enriches surface waters to a certain extend with iron. Hence, as soon as the conditions are favourable for DMSP

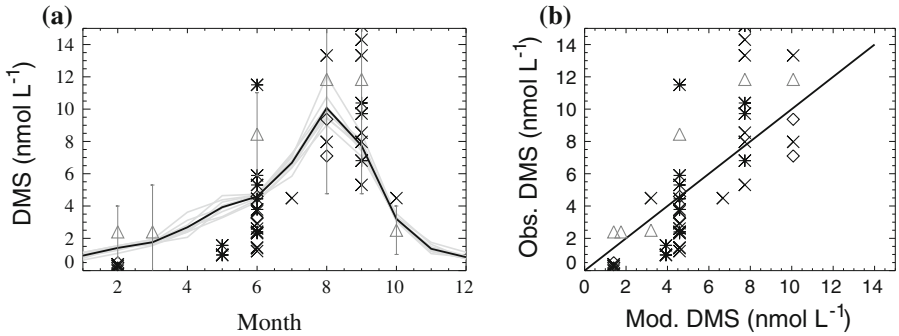

Fig. 8 **a** and **b** as Fig. 6b and c with model results from a test run with seasonally varying S:N ratio to represent the absence of dinoflagellates in winter and spring

producing phytoplankton, we would expect the DMS concentration to increase with increased phytoplankton production and increased zooplankton grazing. The phytoplankton would eventually be grazed down (as observed for example during SERIES Levasseur et al. 2006; as observed for example during SERIES Steiner and Denman 2008) or dispersed by a new mixing event. Such a cycle would be repeated as soon as the winds calm down and the surface warms up again. The model does not represent the iron enrichment, but the weaker iron limitation allows for intensified growth during favourable conditions. The simulation shows later in summer with decreasing mixing depths, the spikes become less pronounced and subside in fall when temperatures and general production decrease.

While low winds and shallow mixed layers are generally correlated, high irradiances and shallow mixed layers are not necessarily so. Hence, on some occasions high irradiances occur with higher winds and deeper mixed layers, in which cases no pronounced DMS peak is present. In case of shallow mixed layers and fairly normal irradiances, a DMS peak still occurs, however less pronounced than if accompanied by a strong irradiance signal as well (e.g., as after day 166 in Fig. 7). This might explain why empirical formulations of DMS as function of mixed layer (e.g., Simó and Dachs 2002) or irradiance (e.g., Vallina and Simo 2007) work in some occasions and not in others (e.g., Asher et al. 2011).

Sporadic natural iron fertilization at OSP, which can also be short term and regionally limited, is not infrequent (see section "Biology and physics of the study area") and can cause interannual variability, however is not likely responsible for a long term trend.

Natural iron fertilization in September 2008

An anomalous widespread phytoplankton bloom fuelled by volcanic ash was detected in the subarctic northeast Pacific in August 2008 (Hamme et al. 2010) and intense CO_2 drawdown was noted by moored instruments at OSP from August 13–17 (http://www.pmel.noaa.gov/co2/moorings/papa). Within the regular Line P fall cruise the DFO ship reached OSP about 8 days after the onset of the CO_2 drawdown. However, measurements from August 21 show fairly regular DMS concentration despite higher phytoplankton biomass, and low but higher than normal relative contributions of diatoms as determined from HPLC pigment analysis (Fig. 5). Results of the SERIES experiment in 2002 have shown that iron fertilization stimulated a bloom of all phytoplankton groups, starting with an increase in biomass of all pico- and nanophytoplankton followed by a bloom of large diatoms (e.g., Harrison 2006, and references therein). The small phytoplankton bloom during the first 8 days, coincided with an increase in surface particulate DMSP. In the week after the small phytoplankton bloom DMS concentrations decreased until they were less than outside the patch (Levasseur et al. 2006; Merzouk et al. 2006). A similar response can be expected for natural iron fertilization. Hence, we applied the model, which has been tested for the SERIES experiment (Steiner et al. 2007), for the respective time period and fertilized (via a lift of the iron limitation in the phytoplankton growth function) on August 13. In correspondence with the SERIES observations DMSP production is highest during the small phytoplankton bloom and DMS production increases during the phase of intense zooplankton grazing. Hence, the DMS peak occurs shortly after the peak in small phytoplankton biomass. With the decrease of the bloom and decreased zooplankton grazing, DMS concentrations reduce until they reach values below regular. The model results suggest that the ship arrived at OSP (August 21) at a time when the initially triggered small phytoplankton bloom has died down due to zooplankton grazing and the following diatom bloom has not yet fully developed (Fig. 9b–d). By that time, DMS concentrations have been reaching fairly regular values again (Fig. 9a).

Summary

About a decade of DMS observations along Line P and at OSP have been summarized and analyzed in terms of seasonal and interannual patterns and compared with model simulations for 2002–2010. The data indicate high spatial and temporal variability which makes it difficult to draw a conclusive picture.

Earlier measurements show an increase in DMS concentrations from coastal stations to the open ocean regime, while more recent measurements suggest this to be indicative of the summer situation; and that the longitudinal concentration gradient reverses seasonally, with highest values occurring offshore in summer.

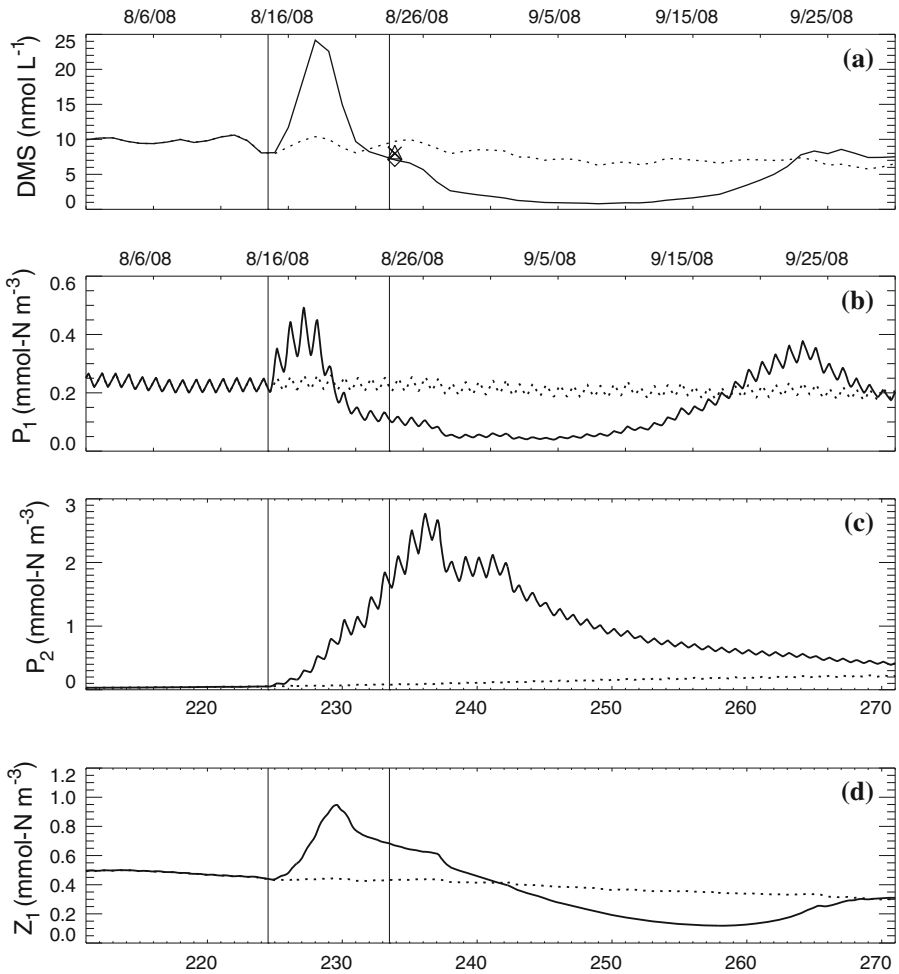

Fig. 9 Model simulations for the natural iron fertilization in the eastern North Pacific in August 2008. *Solid line* shows a model run fertilized with iron (via a lift of the iron limitation in the phytoplankton growth function (Steiner et al. 2006)) on August 13 (*first vertical line*), *dotted line* shows the standard run without fertilization. The model results suggest that when the ship arrived at OSP (August 21st, *second vertical line*) the initially triggered small phytoplankton bloom has died down and the following diatom bloom has not yet fully developed. **a** Simulated DMS (nmol l^{-1}) and measurements on August 21 (top 20 m average and surface data from bottle casts, *cross* and *triangle*, and averaged MIMS data, *diamond*). **b** Simulated small phytoplankton (P_1), **c** diatoms (P_2) and **d** small zooplankton (Z_1). Latter all in mmol-N m^{-3}

In spring, offshore values are typically much lower and the gradient less steep. During the late 1990s El Niño, the spring observations were much higher and the longitudinal concentration gradient more representative of a summer condition. DMS profiles at OSP confirm that the low spring DMS concentrations seen in recent years are comparable to some earlier measurements, e.g., in 1996, and that higher spring values are likely caused by unusual forcing conditions (e.g., ENSO).

Following an analysis of the HPLC data, we suggest that in usual years the contribution of DMSP producing phytoplankton species to the small phytoplankton group is lower in spring (May/June), mainly due to the absence of dinoflagellates, which causes lower DMS concentrations. Concentrations increase later in summer, when prymnesiophytes and dinoflagellates dominate the small phytoplankton size class and DMS production rates are highest (late August early September). In occasional years, a phytoplankton bloom might be triggered earlier in the year causing increased DMS concentrations already in spring (e.g., in 2005). In those years DMS concentrations tend to be lower in summer. DMS concentrations decline in late September due to reduced production and are at a minimum in winter.

The modelled annual cycle which has been calibrated to simulate earlier DMS measurements (1996–2001) is in its current configuration not able to represent the more recent lower values in spring, nor the reduced concentrations observed in winter (February, now below 1 nM compared to 1–3 nM in the late 1990s and early 2000). Simulated summer concentrations are still in good correspondence with the observations. The model suggests, that physical forcing alone cannot be responsible for the observed change. We find that a large part of the differences between model and data are related to biological factors, most likely the representation of the phytoplankton assemblage. The model currently simulates two phytoplankton size classes. This does not account for changes within size classes, e.g., observed differences in the seasonal cycle of the DMS producing species prymnesiophytes and dinoflagellates. To account for this, the S:N ratio within small phytoplankton needs to vary seasonally. Representing the lower ratio of DMSP producing species to non-DMS producing species in winter and spring compared to summer requires either to explicitly resolve dinoflagellates as an individual phytoplankton class or to impose a seasonal cycle in DMS models.

Model simulations link interannual changes in DMS maxima and short term variability to wind mixing, stratification and irradiance, especially in spring and early summer. An example is given for 2005 and 2006, with 2005 showing an early and consistent DMS increase in spring following consistent low winds, shallow mixed layers and high irradiances; and 2006 showing sporadic peaks of high DMS concentrations following episodes of strong and deep mixing all through spring and early summer. Changes like this might be influenced by decadal climate signals like the PDO or ENSO in years with exceptionally high indices. However, at this point a consistent correlation can not be detected. The model simulates a larger amplitude of the short term variability when DMSP producing phytoplankton species are less iron limited.

Natural iron fertilization can cause anomalies as well, however, those are usually short term (<1 month) and regionally limited and can only be represented in the model when specified in advance. For example, a simulation of the volcano triggered bloom in August 2008 shows that the initiated DMS increase subsides after $\sim$8 days, before the diatom bloom reaches its full expansion (and the satellite observed chlorophyll signal reaches its maximum).

This overview of DMS data in the NE Pacific emphasizes the variability at every scale. While the timeseries spans over 15 years, the limitations of these kind of measurements are apparent, adding layers of complexity and challenges to the development of DMS ecosystem models. The data shows large spatial and temporal variability and measurements are fairly localized (although MIMS measurements now allow for better averaging at the surface). Annual variations in cruise timing make it difficult to differentiate between seasonal and interannual signals.

Models are helpful tools, which allow us to study seasonal and interannual cycles as well as interactions between physics and biology. However, model calibration with limited data and lacking rate measurements is challenging. While we continue to learn both from the models ability to represent observations as well as from its limitations, the study points out the necessity of regular model validation, reevaluation of model components and parameter optimization. The continuation of DMS measurements as part of the standard Line P and OSP monitoring program, as well as improvements and new developments in measurement techniques (e.g., MIMS, HPLC) will help to decrease the error margins in model and data intercomparisons and allow for the model to shed light into the gaps caused by limited observations.

Acknowledgements We thank Martine Lizotte, C.S. Wong and Emmy Wong for their involvement in the DMS timeseries, Nina Nemcek for the analysis of HPLC samples, Lizzy Asher for sharing her insights into the MIMS data, and Ken Denman for his contributions to the development of the DMS model. We are grateful to the officers and crew of the CCGS John P. Tully for their assistance and cooperation. NCEP reanalysis data were kindly prepared by Steve Lambert. Argo data interpolated to OSP were kindly prepared by Howard Freeland. The latter were collected and made freely available by the International Argo project and the national programs that contribute to it (http://www.argo.ucsd.edu, http://argo.jcommops.org). The work was supported by grants from the Natural Sciences and Engineering Research Council (NSERC)(M. Levasseur, P. Tortell), as well as contributions from Environment Canada and from Fisheries and Oceans Canada.

References

Archer D, Emerson S, Powell T, Wong C (1993) Numerical hindcasting of sea surface pCO_2 at weathership Station Papa. Prog Oceanogr 32:319–351

Asher EC, Merzouk A, Tortell P (2011) Fine-scale spatial and temporal variability of surface water Dimethylsufide

(DMS) concentrationsand sea-air fluxes in the NE Subarctic Pacific. Mar Chem 126(1–4):63–75. doi:10.1016/j.marchem.2011.03.009

Belviso S, Bopp L, Moulin C, Orr JC, Anderson T, Aumont O, Chu S, Elliot S, Maltrud ME, Simó R (2004) Comparison of global climatological maps of sea surface dimethyl sulfide. Glob Biogeochem Cycles 18:GB3013. doi:10.1029/2002GB002193

Booth B, Lewin J, Postel J (1993) Temporal variation in the structure of autotrophic and heterotrophic communities in the sub-arctic Pacific. Prog Oceanogr 32(1–4):57–99

Boyd P, Harrison P (1999) Phytoplankton dynamics in the NE subarctic Pacific. Deep Sea Res II 46:2405–2432

Boyd P, Wong C, Merill J, Whitney F, Snow J, Harrison P, Gower J (1998) Atmospheric iron supply and enhanced vertical carbon flux in the NE subarctic Pacific: is there a connection. Glob Biogeochem Cycles 12(3):429–441

Boyd P, Law C, Wong C, Nojiri Y, Tsuda A, Levasseur M, Takeda S, Rivkin R, Harrison P, Strzepek R, Gower J, McKay M, Abraham E, Arychuk M, Barwell-Clarke J, Crawford W, Hale M, Harada K, Johnson K, Kiyosawa H, Kudo I, Marchetti A, Miller W, Needoba J, Nishioka J, Ogawa H, Page J, Robert M, Saito H, Sastri A, Sherry N, Soutar T, Sutherland N, Taira Y, Whitney F, Wong SKE, Yoshimura T (2004) The decline and fate of an iron-induced subarctic phytoplankton bloom. Nature (428): 549–552

Burchard H, Bolding K, Villarreal MR (1999) GOTM–a general ocean turbulence model. Theory, applications and test cases. Tech Rep EUR 18745 EN, European Commission

Campolongo F, Gabric A (1997) The parametric sensitivity of dimethylsulfide flux in the southern ocean. J Stat Comput Simul 57:337–352

Cropp RA, Norbury J, Gabric AJ, Braddock RD (2004) Modeling dimethylsulphide production in the upper ocean. GlobBiogeochem Cycles 18:GB3005. doi:10.1029/2003GB002126

Denman KL, Miyake M (1973) Upper layer modification at Ocean Station Papa: observations and simulation. J Phys Oceanogr 3:185–196

Denman KL, Voelker C, Peña MA, Rivkin RB (2006) Modelling the ecosystem response to iron fertilization in the subarctic NE Pacific: the influence of grazing, and Si and N cycling on CO_2 drawdown. Deep Sea Res II 53:2105–2121

DFO (2009) State of the Pacific Ocean 2009. Tech Rep 2010/034, DFO Can Sci Advis Sec Sci Advis Rep

Freeland HJ, Cummins PF (2005) Argo: a new tool for environmental monitoring and assessment of the world's oceans, an example from the N.E. Pacific. Prog Oceanogr 64:31–44

Halloran P, Bell T, Totterdell I (2010) Can we trust empirical marine DMS parameterisations within projections of future climate. Biogeosciences 7:1645–1656. doi:10.5194/bg-7-1645-2010

Hamme RC, Webley PW, Crawford WR, Whitney FA, DeGrandpre MD, Emerson SR, Eriksen CC, Giesbrecht KE, Gower JFR, Kavanaugh MT, Peña MA, Sabine CL, Batten SD, Coogan LA, Grundle DS, Lockwood D (2010) Volcanic ash fuels anomalous plankton bloom in subarctic Northeast Pacific. Geophys Res Lett 37:L19604. doi:10.1029/2010GL044629

Harrison P (2006) SERIES (subarctic ecosystem response to iron enrichment study): a Canadian–Japanese contribution to our understanding of the iron-ocean-climate connection. Deep Sea Res II 53:2006–2011

Harrison P, Boyd P, Varela D, Takeda S, Shiomoto A, Odate T (1999) Comparison of factors controlling phytoplankton productivity in the NE and NW subarctic Pacific gyres. Prog Oceanogr 43:205–234

Jackson JM, Myers PG, Ianson D (2006) An examination of advection in the northeast Pacific Ocean 2001–2005. Geophys Res Lett 33:L15601. doi:10.1029/2006GL026278

Johnson WK, Miller LA, Sutherland NE, Wong C (2005) Iron transport by mesoscale Haida eddies in the Gulf of Alaska. Deep Sea Res II 52:933–953

Kalnay E, Kanamitsu M, Kistler R, Collins W, Deaven D, Gandin L, Iredell M, Saha S, White G, Woolen J, Zhu Y, Leetma A, Reynolds R, Chelliah M, Ebisuzaki W, Higgins W, Janowiak J, Mo K, Ropelewski C, Wang J, Jenne R, Josef D (1996) The NCEP/NCAR 40-year reanalysis project. Bull Am Meteorol Soc 77:437–471

Keller M, Bellows W, Guillard R (1989) Dimethyl sulfide production in marine phytoplankton. Am Chem Soc Symp Ser 393:167–182

Lam PJ, Bishop JK, Henning CC, Marcus MA, Waychunas GA, Fung IY (2006) Wintertime phytoplankton bloom in the subarctic Pacific supported by continental margin iron. Glob Biogeochem Cycles 20:GB1006. doi:10.1029/2005GB002557

Lana A, Bell T, Simo R, Vallina SM, Ballabrera-Poy SV, Kettle AJ, Dachs J, Bopp L, Saltzman E, Stefels J, Johnson J, Liss P (2011) An updated climatology of surface dimethylsulphide concentrations and emission fluxes in the global ocean. Glob Biogeochem Cycles 25:GB1004. doi:10.1029/2010GB003850

Le Clainche Y, Levasseur M, Vézina A, Bouillon RC, Merzouk A, Michaud S, Scarratt M, Wong CS, Rivkin RB, Boyd PW, Harrison PJ, Miller WL, Law CS, Saucier FJ (2006) Modeling analysis of the effect of iron enrichment on dimethylsulfide dynamics in the N.E. Pacific (SERIES experiment). J Phys Oceanogr 111:C01011. doi:10.1029/2005JC002947

Le Clainche Y, Vézina A, Levasseur M, Cropp R, Gunson J, Vallina S, Vogt M, Lancelot C, Allen I, Archer S, Bopp L, Deal C, Elliott S, Jin M, Malin G, Schoemann V, Simó R, Six K, Stefels J (2010) A first appraisal of prognostic ocean DMS models and prospects for their use in climate simulation. Glob Biogeochem Cycles 24:GB3021. doi:10.1029/2009GB003721

Levasseur M, Scarratt M, Michaud S, Merzouk A, Wong CS, Arychuk M, Richardson W, Wong E, Marchetti A, Kivosawa H (2006) DMSP and DMS dynamics during a mesoscale iron fertilization experiment in the Northeast Pacific. Part I. Temporal and vertical distributions. Deep Sea Res II 53:2353–2369

Mackas D, Peterson W, Ohman M, Lavaniegos B (2006) Zooplankton anomalies in the california current system before and during the warm ocean conditions of 2005. Geophys Res Lett 33:L22S07. doi:10.1029/2006GL027930

Martin J, Gordon R, Fitzwater S, Broenkow W (1989) VERTEX: phytoplankton/iron studies in the Gulf of Alaska. Deep Sea Res 36(5):649–680

Merzouk A, Levasseur M, Scarratt MG, Michaud S, Rivkin RB, Hale MS, Kiene RP, Price NM, Li WK (2006) DMSP and DMS dynamics during a mesoscale iron fertilization experiment in the Northeast Pacific. Part II: biological cycling. Deep Sea Res II 53:2370–2383

Monahan AH, Denman KL (2004) Impacts of atmospheric variability on a coupled upper-ocean/ecosystem model of the subarctic northeast Pacific. Glob Biogeochem Cycles 18:GB2010. doi:10.1029/2003GB002100

Moore J, Doney S, Glover D, Fung I (2002) Iron cycling and nutrient-limitation patterns in surface waters of the world ocean. Deep Sea Res II 49:463–507

Nishioka J, Takeda S, Wong C, Johnson W (2001) Size-fractionated iron concentrations in the northeast Pacific Ocean: distribution of soluble and small colloidal iron. Mar Chem 74:157–179

Nishioka J, Takeda S, Kudo I, Tsumune D, Yoshimura T, Kuma K, Tsuda A (2003) Size-fractionated iron distributions and iron-limitation processes in the subarctic NW Pacific. Geophys Res Lett 30(14):1730. doi:10.1029/2002GL016853

Peña MA, Varela DE (2007) Seasonal and interannual variability in phytoplankton and nutrient dynamics along Line P in the NE subarctic Pacific. Prog Oceanogr 75(2): 200–222. doi:10.1016/j.pocean.2007.08.009

Royer SJ, Levasseur M, Lizotte M, Arychuk M, Scarratt MG, Wong CS, Lovejoy C, Robert M, Johnson K, Peña A, Michaud S, Kiene RP (2010) Microbial dimethylsulfoniopropionate (DMSP) dynamics along a natural iron gradient in the northeast subarctic pacific. Limnol Oceanogr 55(4):1614–1626. doi:10.4319/lo.2010.55.4.1614

Schäfer H, Myronova N, Boden R (2010) Microbial degradation of dimethylsulfide and related c1-sulfur compounds: organisms and pathways controlling fluxes of sulfur in the biosphere. J Exp Bot 61:315–334. doi:10.1093/jxb/erp355

Simó R, Dachs J (2002) Global ocean emission of dimethylsulfide predicted from biogeophysical data. Glob Biogeochem Cycles 16(4):1018. doi:10.1029/2001GB001829

Six KD, Maier-Reimer E (2006) What controls the oceanic dimethylsulfide (DMS) cycle. Glob Biogeochem Cycles 20:GB4011. doi:10.1029/2005GB002674

Stefels J, Steinke M, Turner S, Malin G, Belviso S (2007) Environmental constraints on the production and removal of the climatically active gas dimethylsulfide (DMS) and implications for ecosystem modelling. Biogeochemistry 83(1–3), 245–275. doi:10.1007/s10533-007-9091-5

Steiner N, Denman K (2008) Parameter sensitivities in a 1-d model for DMS and sulphur cycling in the upper ocean. Deep Sea Res I 55:847–865

Steiner N, Denman K, McFarlane N, Solheim L (2006) Simulating the atmosphere-ocean physical conditions and effects on the planktonic ecosystem response during SERIES. Deep Sea Res II 53:2434–2454

Steiner N, Vagle S, Denman K, McNeil C (2007) Oxygen and nitrogen cycling in the Northeast Pacific—simulations and observations at station Papa in 2003/2004. J Mar Res 65(3):441–469

Tortell PD (2005) Dissolved gas measurements in oceanic waters made by membrane inlet mass spectrometry. Limnol Oceanogr 3:24–37

Vallina S, Simo R (2007) Strong relationship between DMS and the solar radiation dose over the global surface ocean. Science 315:506–508

Varela D, Harrison P (1999) Seasonal variability in nitrogenous nutrition of phytoplankton assemblages in the northeastern subarctic Pacific Ocean. Deep Sea Res II 46:2505–2538

Vézina A (2004) Ecosystem modelling of the cycling of marine dimethylsulfide: a review of current approaches and of the potential for extrapolation to global scales. Can J Fish Aquat Sci 61:845–856

von Salzen K, McFarlane N, Lazare M (2005) The role of shallow convection in the water and energy cycles of the atmosphere. Climate Dyn 25:671–688

Whitney FA, Crawford DW, Yoshimura T (2005a) The uptake and export of silicon and nitrogen in HNLC waters of the NE Pacific Ocean. Deep Sea Res II 52:1055–1067

Whitney FA, Crawford WR, Harrison PJ (2005b) Physical processes that enhance nutrient transport and primary productivity in the coastal and open ocean of the subarctic NE Pacific. Deep Sea Res II 52:681–706

Wong CS, Wong SE, Richardson WA, Smith GE, Arychuk MD, Page JS (2005) Temporal and spatial distribution of dimethylsulfide in the subarctic northeast Pacific Ocean: a high-nutrient-low-chlorophyll region. Tellus 57:317–331

Wong C, Wong SK, Peña A, Levasseur M (2006) Climatic effect on DMS producers in the NE sub-arctic Pacific: ENSO on the upper ocean. Tellus 58:319–326